JOC The Journal of Organic Chemistry

Article

pubs.acs.org/joc

Tandem β-Elimination/Hetero-Michael Addition Rearrangement of an N-Alkylated Pyridinium Oxime to an O-Alkylated Pyridine Oxime Ether: An Experimental and Computational Study

Igor Picek,*[,†] Robert Vianello,*[,‡] Primož Šket,[§,∥] Janez Plavec,[§,∥,⊥] and Blaženka Foretić*[,†]

[†]Department of Chemistry and Biochemistry, University of Zagreb, School of Medicine, Šalata 3, HR-10000 Zagreb, Croatia

[‡]Division of Organic Chemistry and Biochemistry, Ruđer Bošković Institute, Bijenička 54, HR-10000 Zagreb, Croatia

[§]Slovenian NMR center, National Institute of Chemistry, Hajdrihova 19, SI-1000 Ljubljana, Slovenia

[∥]EN-FIST Centre of Excellence, Trg Osvobodilne fronte 13, SI-1000 Ljubljana, Slovenia

[⊥]Faculty of Chemistry and Chemical Technology, University of Ljubljana, Aškerčeva cesta 5, SI-1000 Ljubljana, Slovenia

Supporting Information

ABSTRACT: A novel OH^--promoted tandem reaction involving C(β)−N^+(pyridinium) cleavage and ether C(β)−O(oxime) bond formation in aqueous media has been presented. The study fully elucidates the fascinating reaction behavior of *N*-benzoylethylpyridinium-4-oxime chloride in aqueous media under mild reaction conditions. The reaction journey begins with the exclusive β-elimination and formation of pyridine-4-oxime and phenyl vinyl ketone and ends with the formation of O-alkylated pyridine oxime ether. A combination of experimental and computational studies enabled the introduction of a new type of rearrangement process that involves a unique tandem reaction sequence. We showed that (*E*)-*O*-benzoylethylpyridine-4-oxime is formed in aqueous solution by a base-induced tandem β-elimination/hetero-Michael addition rearrangement of (*E*)-*N*-benzoylethylpyridinium-4-oximate, the novel synthetic route to this engaging target class of compounds. The complete mechanistic picture of this rearrangement process was presented and discussed in terms of the E1cb reaction scheme within the rate-limiting β-elimination step.

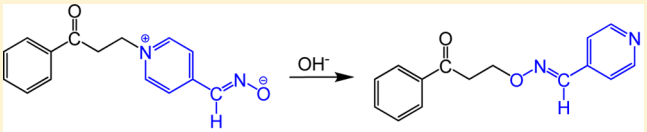

N-Benzoylethylpyridinium-4-oximate *O*-Benzoylethylpyridine-4-oxime ether

INTRODUCTION

Over the last few decades, the reactivity of oxime nucleophiles has attracted considerable attention, primarily aimed at mimicking the catalytic mode of hydrolytic enzymes and realizing efficient artificial catalysts.[1] The oxime group, especially on incorporation into a positively charged pyridinium aromatic system, is known to be an exceptionally effective nucleophile. Consequently, many acidic pyridinium oximes (pK_a values around 7−9) are pharmacologically well-known esterolytic agents used as reactivators of the enzyme acetylcholinesterase initially inhibited by organophosphorus poisons, such as pesticides and nerve gases.[2,3] In recent years, there has been a growing interest in the utility of oximes as oxygen nucleophiles (Michael donors) in the selective synthesis of O-substituted pyridine oxime ethers, currently attractive synthetic target molecules used in the molecular design of drugs because of their considerable application potential in medicinal and bioorganic chemistry.[4−6] The conventional methods for the synthesis of O-substituted oxime ethers have been based on the base-catalyzed reactions of the respective pyridine oximes with alkyl and aryl halides or on multicomponent one-pot synthesis using carbonyl-, halogen-, and cyano-pyridine derivatives.[7] Novel methods based on transition metal or organo catalyzed Michael additions of oximes to activated[8−10] or nonactivated[11,12] unsaturated Michael acceptors in nonaqueous solutions have been developed.

As part of our ongoing research program aimed at investigating the pentacyanoferrate(II) complexes of pharmacologically active pyridinium-4-oxime derivatives,[13] our recent research has been focused on the comparative structural studies of the *N*-phenacyl and *N*-benzoylethyl derivatives of pyridinium and pyridinium-4-oxime in aqueous solutions.[14] The investigation of the stability of these compounds in mild and highly alkaline media revealed substantial differences in their reactivity. One can reasonably assume that, under these conditions, the focus would be on the reactivity of the carbonyl group, and this was true in the case of the *N*-phenacyl derivatives and the *N*-benzoylethylpyridinium cation, where the structural perturbations were initialized by the addition of the hydroxide ion to the carbonyl group. The striking result was that this kind of reactivity was not observed with the *N*-benzoylethylpyridinium-4-oxime cation. It was recognized that the *N*-benzoylethylpyridinium-4-oximate zwitterion was the reactive form, subjected to β-elimination followed by the formation of a novel compound at a higher pH. This unexpected outcome encouraged us to expand the study of the *N*-benzoylethylpyridinium-4-oxime behavior to identify the novel

Received: November 24, 2014
Published: January 6, 2015

ACS Publications © 2015 American Chemical Society

DOI: 10.1021/jo5026755
J. Org. Chem. 2015, 80, 2165−2173

Scheme 1. Rearrangement of (*E*)-*N*-Benzoylethylpyridinium-4-oximate to (*E*)-*O*-Benzoylethylpyridine-4-oxime and Structures of the Other Ionic Forms Involved

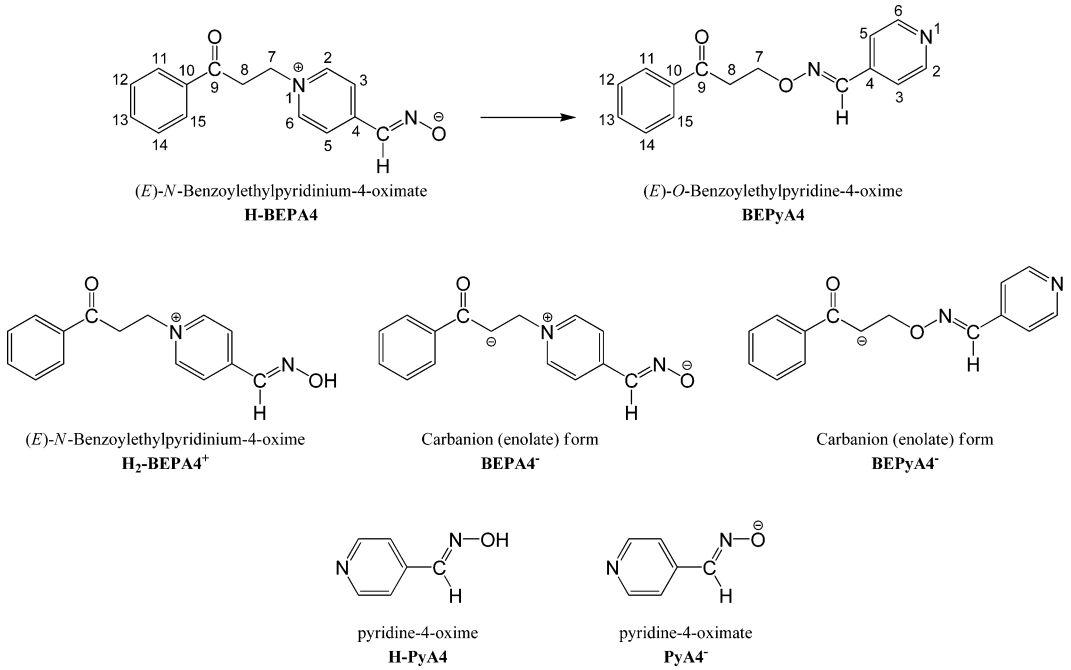

compound and to resolve the mechanistic aspects of its formation.

In this study we describe the identification and structural characterization of the new O-alkylated pyridine oxime ether formed by the rearrangement of the corresponding N-substituted pyridinium oxime in aqueous solution (Scheme 1). By combining experimental and computational efforts, we also provide insight into the complete mechanism of this novel reaction.

RESULTS AND DISCUSSION

Identification of O-Alkylated Pyridine Oxime Ether. The novel compound was, due to its lower aqueous solubility, isolated from a highly alkaline solution of **H_2-BEPA4**$^+$ (details are presented in the Experimental Section). The results of the elemental and MS analysis of the crude product indicated a chemical composition equivalent to the **H-BEPA4** zwitterion, whereas the FT-IR spectrum showed the typical acetophenonic C═O stretching band and strongly attenuated oximic C═N stretching (Figure S1 (Supporting Information)). The relatively low melting point of 87.8 °C indicated an uncharged structure for the compound. To elucidate the structure, ^{1}H and ^{13}C CP-MAS solid-state NMR measurements were performed. In the ^{1}H MAS NMR spectrum (Figure S2a (Supporting Information)) the signals at δ 4.3 and 3.0 ppm and over the range of δ 6.5−8.5 ppm indicated the presence of ethylene and aromatic protons within the structure. The signals at δ 197 and 164 ppm in the ^{13}C CP-MAS spectrum (Figure S2b (Supporting Information)) suggested the presence of benzoyl and oxime groups, respectively. Aromatic carbons were observed between δ 115 and 152 ppm, and signals of an ethylene group resonated at δ 36 and 71 ppm. It is interesting to note that one of the signals corresponding to the carbon atoms of the ethylene group exhibited an unusually high chemical shift value, pointing to its proximity to the atom more electronegative than pyridinium nitrogen. To evaluate this high chemical shift value, the ^{1}H−^{13}C gHSQC, ^{1}H−^{13}C gHMBC, gCOSY, and ^{1}H−^{15}N gHMBC spectra were acquired. In the ^{1}H−^{13}C HMBC spectrum, the H7 and H8 protons of the ethylene group showed two-bond correlations to the respective ethylene carbons and to the carbonyl atom C9. However, in the ^{1}H−^{15}N HMBC spectrum, the nitrogen atom of the oxime group exhibited a correlation to the H7 ethylene protons and to the proton on the oximic carbon atom. The pyridine nitrogen atom showed correlations only to the aromatic protons of the pyridine ring.

These results confirmed that the final structure was in accordance with the O-alkylated pyridine oxime ether *O*-benzoylethylpyridine-4-oxime (**BEPyA4**), as shown in Scheme 1.

Moreover, a single set of NMR signals in the ^{1}H and ^{13}C NMR spectra of **BEPyA4** suggested that it was isolated solely as one configurational stereoisomer. The excellent analogy in the selected ^{1}H and ^{13}C chemical shifts of **BEPyA4** (8.60 (d, J = 5.94 Hz, 2H), 8.22 (s, 1H), 120.8, 147.3, 150.2 ppm) with those of (*E*)-pyridine-4-oxime (**H-PyA4**) (8.60 (d, J = 6.00 Hz, 2H), 8.18 (s, 1H), 120. 8, 146.9, 150.3 ppm) in [D_6]DMSO confirmed that **BEPyA4** was formed exclusively as the *E* stereoisomer.

Reactive Intermediates during Formation of BEPyA4. Because several reaction pathways leading to the formation of **BEPyA4** are possible, NMR studies of the reaction mixtures were performed at pH >10 to establish the exact reaction sequence (see the Experimental Section and Table S1 (Supporting Information)). The qualitative analysis was performed by comparison with the known chemical shifts for **H-PyA4**, phenyl vinyl ketone (**PVK**),[15] **H_2-BEPA4**$^+$,[16] and **BEPyA4**. The ^{13}C NMR chemical shift values, especially those corresponding to the carbonyl signals at δ 190.0 and 197.9 ppm, were consistent with the presence of **PVK** and **BEPyA4**. The identification of **PVK** was additionally supported by the three doublets of doublets observed at δ 5.97, 6.32, and 7.38 ppm in the ^{1}H NMR spectrum, originated from the coupling of the geminal, cis, and trans protons within the vinyl group of **PVK**. The identification of the

DOI: 10.1021/jo5026755
J. Org. Chem. 2015, 80, 2165−2173

second reaction intermediate, **H-PyA4**, was based on the distinctive sets of ^{1}H NMR signals at δ 8.17, 8.60, and 12.13 ppm and ^{13}C NMR signals at δ 120.6, 140.4, 146.4, and 150.1 ppm. The identified reaction participants clearly discriminated the reaction pathway and confirmed that **BEPyA4** is formed by the two-reaction sequence consisting of β-elimination with the formation of **H-PyA4** and **PVK** and the subsequent hetero-Michael addition of pyridine-4-oximate (**PyA4**$^-$) to **PVK**. This pH-dependent rearrangement is controlled by the concentration of **PyA4**$^-$, which, as a strong oxygen nucleophile, predominates in solution at pH >10 (pK_a(**H-PyA4**) = 9.99[17]).

Kinetic Studies of the Rearrangement. The kinetic studies were performed in the single-base OH^-/H_2O and OH^-/H_2O/EtOH systems, the two-base glycine buffer system $OH^-/GLY^-/H_2O$, and the multiple-base Britton–Robinson buffer (BRB) system. All of the kinetic experiments were performed in alkaline aqueous media up to a pH of 11.5, avoiding a higher pH to suppress the microscopic reverse of the Michael addition: i.e., the β-elimination of **BEPyA4**. In fact, the performed time-dependent electron absorption studies of the **BEPyA4** solutions showed that β-elimination was plausible at pH $\geq$11.5.

Reaction Activation Parameters and Solvent Effects. On the basis of the fact that β-elimination was the exclusive reaction in the pH range 7–10[14] and tandem β-elimination/hetero-Michael addition occurred at pH >10, two kinetic experiments were conducted to elucidate the rate-limiting step: determination of the reaction activation parameters in the OH^-/H_2O and the BRB systems (Table 1 and Table S2 (Supporting Information)) and

Table 1. Thermodynamic Activation Parameters $\Delta H^{\ddagger}$ (kcal mol^{-1}), $\Delta S^{\ddagger}$ (cal K^{-1} mol^{-1}), and $\Delta G^{\ddagger}$ (kcal mol^{-1}) in the OH^-/H_2O and BRB Systems at I = 0.1 M

pH	$\Delta H^{\ddagger}$	$\Delta S^{\ddagger}$	$\Delta G^{\ddagger b}$
	OH^-/H_2O[a] System		
10.0	16.2 ± 0.6	−15.5 ± 1.9	20.9 ± 0.3
10.5	15.6 ± 0.4	−13.5 ± 1.5	19.6 ± 0.6
11.0	15.8 ± 0.2	−10.2 ± 1.8	18.8 ± 0.2
11.5	14.0 ± 0.4	−14.2 ± 1.5	18.2 ± 0.2
	BRB[a] System		
8.3[c]	18.1 ± 0.6	−10.4 ± 2.0	21.2 ± 1.2
9.5[c]	18.3 ± 0.3	−7.4 ± 1.1	20.5 ± 0.5
10.5	18.2 ± 0.2	−4.7 ± 0.9	19.6 ± 0.4
11.2	13.8 ± 0.8	−16.3 ± 2.9	18.7 ± 1.7

[a]The drift in the temperature measurements was ±0.1 °C. [b]The $\Delta G^{\ddagger}$ values were calculated at 298 K using the relationship $\Delta G^{\ddagger} = \Delta H^{\ddagger} - T\Delta S^{\ddagger}$. [c]The exclusive β-elimination of H-BEPA4 occurred.[14]

examination of the solvent polarity on the rearrangement reaction rate in the OH^-/H_2O/EtOH systems at pH 11.0 (Table S3 (Supporting Information)). The inspection of the $\Delta H^{\ddagger}$ and $\Delta G^{\ddagger}$ values determined in the BRB system provided strong evidence that the same type of transition state was formed in the pH range 8.3–11.2 and revealed base-induced β-elimination as the rate-limiting step. Although the smaller value of $\Delta H^{\ddagger}$, determined at pH 11.2 in the BRB system, could suggest a change in the rate-limiting step, the similar $\Delta H^{\ddagger}$ value obtained in the OH^-/H_2O system at pH 11.5 ruled out this possibility and indicated OH^- as the exclusive base involved in the β-elimination. This conclusion is consistent with the observed substantial increase in the reaction rate with a decrease in the solvent polarity, which strongly implicated the association of OH^- with **H-BEPA4**, thus confirming β-elimination as a key kinetic step. The decrease in the solvent polarity increased the OH^- activity by reducing the extent of its stabilization by solvation, making it more accessible to the acid–base reaction. Furthermore, the activation parameters determined in the OH^-/H_2O system strongly supported the consistency of the reaction mechanism within the pH range 10–11.5. The $\Delta S^{\ddagger}$ values were all negative, which is consistent with the associative mechanism of the rate-limiting β-elimination step. In addition, the experimental $\Delta G^{\ddagger}$ values for the OH^-/H_2O system (Table 1) were in excellent agreement with those obtained by the computational study (see below).

Therefore, the overall rearrangement mechanism was considered and discussed through the β-elimination mechanistic model.

Mechanistic Model of Rate-Limiting β-Elimination. The E1cb elimination mechanism with **H-BEPA4** as the exclusive reactive form subjected to β-elimination was assumed to be the most plausible kinetic model (Scheme 2). E1cb is a two-step

Scheme 2. Overall Mechanistic Pathway for the Intramolecular Tandem β-Elimination/Hetero-Michael Addition Rearrangement

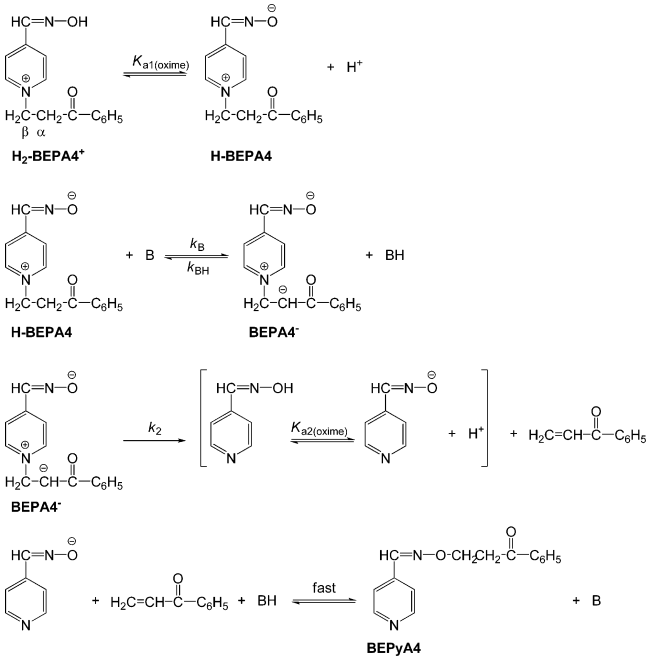

mechanism which involves a reversible ($(E1cb)_R$) or irreversible ($(E1cb)_I$) base-induced formation of a stabilized carbanion intermediate followed by the unimolecular loss of the leaving group. The distinct carbanion intermediate represents the key difference between E1cb and concerted E2 elimination mechanisms. Although the concerted E2 and $(E1cb)_I$ mechanisms cannot be kinetically distinguished, the $(E1cb)_I$ and $(E1cb)_R$ mechanisms can be discriminated by the values of kinetic parameters k_B, k_{BH}, and k_2 (Scheme 2).

Namely, the electronic features of **H-BEPA4** enable an effective stabilization of the carbanion intermediate, **BEPA4**$^-$, by resonance stabilization and the inductive effect. The resonance stabilization is efficiently assisted by the neighboring carbonyl group, whereas the inductive effect is exerted by the proximity of the pyridinium-4-oximate system promoting the electrophilic character of the bonded β-methylene group. In addition, the

DOI: 10.1021/jo5026755
J. Org. Chem. 2015, 80, 2165–2173

important factor of the E1cb mechanism established for the β-elimination of the 2-fluoroethylpyridinium[18] and pyridylethylquinuclidinium salts[19] was the carbanion resonance stabilization or, in the case of *p*-nitrophenylethylquinuclidinium[20] and the substituted *N*,*N*′-ethylenebis(pyridinium)[21] salts, the stabilization of the carbanion by the substituent inductive effect. These factors caused the E1cb mechanism to be energetically favored with respect to the concerted E2 process. The formation of a carbanion intermediate has also been reported in the base-induced β-elimination of N-methylated β-piperidinopropiophenone iodide,[22] a compound having structural characteristics comparable to those of **H-BEPA4**. Furthermore, the enol forms of **H$_2$-BEPA4**$^+$ and **H-BEPA4** and consequent keto−enol equilibria were excluded from consideration since the computational study (see later) showed that both **H$_2$-BEPA4**$^+$ and **H-BEPA4** were the exclusive ionic forms present in solution.

Because the $(E1cb)_I$ and $(E1cb)_R$ intimate mechanisms kinetically differ in the rates of the elementary steps constituting the β-elimination, determination of the key kinetic parameters, independent of the type of aqueous system used, was acquired. These kinetic parameters according to Scheme 2 were as follows: k_B (i.e. k_{OH}), the second-order catalytic rate constant for the OH^--induced formation of **BEPA4**$^-$, k_{BH} (i.e. k_{H_2O}), the pseudo-first-order rate constant for the reprotonation of **BEPA4**$^-$ by H_2O, and k_2, the first-order rate constant for the decomposition of **BEPA4**$^-$. The parameters were determined by combining the results obtained from the kinetic study of the rearrangement in the OH^-/H_2O, $OH^-/GLY^-/H_2O$, and BRB systems (Tables S4−S6 (Supporting Information)).

The E1cb kinetic equation corresponding to the rearrangement of **H-BEPA4** to **BEPyA4** in the OH^-/H_2O system is given as

$$k_{obs} = \frac{k_2}{k_{H_2O} + k_2} k_{OH}[OH^-] \quad (1)$$

An excellent linear dependence of k_{obs} vs $[OH^-]$ was obtained (Table S4 and Figure S3 (Supporting Information)), in accordance with eq 1. The line from the origin had a slope of 83.3 M^{-1} s^{-1}, which was equal to the ratio $k_{OH}k_2/(k_{H_2O} + k_2)$. In the case of $(E1cb)_I$, for which the expression $k_2 \gg k_{H_2O}$ is valid, the ratio $k_2/(k_{H_2O} + k_2)$ is equal to 1.

To discriminate between the $(E1cb)_I$ and $(E1cb)_R$ mechanisms, an additional kinetic study in a two-base buffered system, $OH^-/GLY^-/H_2O$, at the constant pH values of 9.80 and 10.40 was performed by varying the total buffer concentration over a 20-fold range (Table S5 (Supporting Information)). Accordingly, the reaction mechanism given in Scheme 2 was supplemented with an additional elementary step, the reversible GLY^--induced formation of **BEPA4**$^-$ with the corresponding kinetic equation (2).

$$k_{obs} = \frac{k_2(k_{GLY}[GLY^-] + k_{OH}[OH^-])}{k_{GLYH}[GLYH] + k_{H_2O} + k_2} \quad (2)$$

The kinetic parameters k_{GLY} and k_{GLYH} represent the second-order catalytic rate constant for the GLY^--induced formation of **BEPA4**$^-$ and the pseudo-first-order rate constant for the reprotonation of **BEPA4**$^-$ by GLYH, respectively. The linear dependence of k_{obs} on $[GLY^-]$ was obtained for both of pH values (Figure S4 (Supporting Information)). In the case of the $(E1cb)_R$ mechanism, when $k_{GLYH}[GLYH] \gg k_2 + k_{H_2O}$ and $k_{GLY}[GLY^-] \gg k_{OH}[OH^-]$, eq 2 simplifies to $k_{obs} = k_2k_{GLY}[GLY^-]/(k_{GLYH}[GLYH])$. Since this relation predicts that the k_{obs} value should remain constant regardless of the buffer concentration, the $(E1cb)_R$ mechanism was ruled out, and $(E1cb)_I$ was considered as the dominant intimate mechanism. Consequently, the kinetic equation that describes the obtained linear relationship, consistent with the $(E1cb)_I$ mechanism ($k_2 \gg k_{GLYH}[GLYH] + k_{H_2O}$), is

$$k_{obs} = k_{GLY}[GLY^-] + k_{OH}[OH^-] \quad (3)$$

The value of the rate constant k_{OH} (85.0 M^{-1} s^{-1}) was calculated from the intercepts obtained at each pH value (5.4×10^{-3} s^{-1} at pH 9.80 and 19.3×10^{-3} s^{-1} at pH 10.40), whereas the value of k_{GLY} was equal to the slope (0.32 M^{-1} s^{-1}). Furthermore, the linear dependences of the k_{obs} value on $[GLY^-]$ with the slope values of the plots independent of the pH confirmed that the reactive form, which undergoes a base-induced β-elimination, is exclusively **H-BEPA4**. In fact, if **H$_2$-BEPA4**$^+$ was subjected to β-elimination, then the expression for k_{obs} would be $k_{obs} = (k_{GLY}(K_{a1}(\mathbf{H_2\text{-}BEPA4^+})_{oxime})/[H^+])[GLY^-] + k_{OH}[OH^-]^-(K_{a1}(\mathbf{H_2\text{-}BEPA4^+})_{oxime})/[H^+]$. In that case, the slope of the plot k_{obs} vs $[GLY^-]$ would depend on the pH (slope = $k_{GLY}(K_{a1}(\mathbf{H_2\text{-}BEPA4^+})_{oxime})/[H^+]$).

The determined k_{OH} value and the calculated k_{H_2O}/k_{OH} ratio of 1.5873×10^4 M were used to determine the rate constants k_2 and k_{H_2O} and the $k_2/(k_{H_2O} + k_2)$ ratio in eq 1, providing the distinction between the $(E1cb)_I$ and $(E1cb)_R$ intimate mechanisms in the OH^-/H_2O system. The k_{H_2O}/k_{OH} ratio was found from the relationship $k_{H_2O}/k_{OH} = K_w/k_{a(\alpha\text{-}CH_2)}$, where $K_w(25\ °C) = 1 \times 10^{-14}$ M^2 and $k_{a(\alpha\text{-}CH_2)} = 6.3 \times 10^{-19}$ M.[23] The ratio $k_2/(k_{H_2O} + k_2)$ in eq 1 was obtained by using the known value of the slope of the linear plot of k_{obs} vs $[OH^-]$. The parameters are summarized in Table 2.

Table 2. Kinetic Parameters k_{OH} (M^{-1} s^{-1}), k_{H_2O} (s^{-1}), and k_2 (s^{-1}) in the OH^-/H_2O System at 25 °C and I = 0.1 M

k_{OH}	k_2	k_{H_2O}	$k_2/(k_{H_2O} + k_2)$
85.0	6.62×10^7	1.35×10^6	0.98

The values of k_{H_2O} and k_2 and the consequent $k_2/(k_{H_2O} + k_2)$ ratio being nearly equal to 1 implied a negligible contribution of the **BEPA4**$^-$ reprotonation by H_2O to the observed reaction rate, which favors the $(E1cb)_I$ mechanism of the rate-limiting β-elimination. Furthermore, the calculated $K_{a2}(\mathbf{H_2\text{-}BEPA4^+})_{\alpha\text{-}CH_2}$ ($pK_a = 17.9$) and k_{H_2O} values were comparable to those estimated for 1-methyl-2-(2-fluorethyl)pyridinium iodide ($pK_a \approx 18$; $k_{H_2O} \approx 10^5$ s^{-1}),[24] which provided supporting evidence for the established $(E1cb)_I$ mechanism. Similarly, values several orders of magnitude higher were found for CH_3CN ($pK_a = 28.9$; $k_{H_2O} \approx 10^{11}$ s^{-1})[25] in which case the reprotonation of the carbanion intermediate by H_2O could not be neglected.

The sustainability of the $(E1cb)_I$ mechanistic model was verified with kinetic experiments conducted on BRB systems in the pH range 7.5−11.3. In the specified pH range, the reaction mixture contained the following bases: OH^-, Ac^-, $H_2PO_4^-$, HPO_4^{2-}, PO_4^{3-}, and $H_2BO_3^-$. The contribution of $H_2PO_4^-$ to the reaction rate was neglected because of its poor base properties (pK_b = 11.85 at 25 °C). Moreover, the identical

DOI: 10.1021/jo5026755
J. Org. Chem. 2015, 80, 2165−2173

values of k_{obs} and activation parameters obtained in the BRB system at pH 11.2 and in the OH^-/H_2O system at pH 11.5 (Table 1 and Tables S4 and S6 (Supporting Information)) were in accordance with the predominant influence of the $k_{OH}[OH^-]$ parameter on the reaction rate and of the insignificant contribution of PO_4^{3-} and $H_2BO_3^-$. Accordingly, the reaction mechanism given in Scheme 2 was supplemented with two additional elementary steps: the reversible Ac^-- and HPO_4^{2-}-induced formation of **BEPA4**$^-$. The corresponding kinetic equation for the k_{obs}, consistent with the $(E1cb)_I$ mechanism is

$$k_{obs} = k_{Ac}[Ac^-] + k_{HPO_4}[HPO_4^{2-}] + k_{OH}[OH^-] \quad (4)$$

where k_{Ac} and k_{HPO_4} are the second-order rate constants for the Ac^-- and HPO_4^{2-}-induced formation of **BEPA4**$^-$, respectively. The best-fitting curve (r^2 = 0.9971) (Figure 1) was obtained by fitting of the experimental points (Table S6 (Supporting Information)) to eq 4.

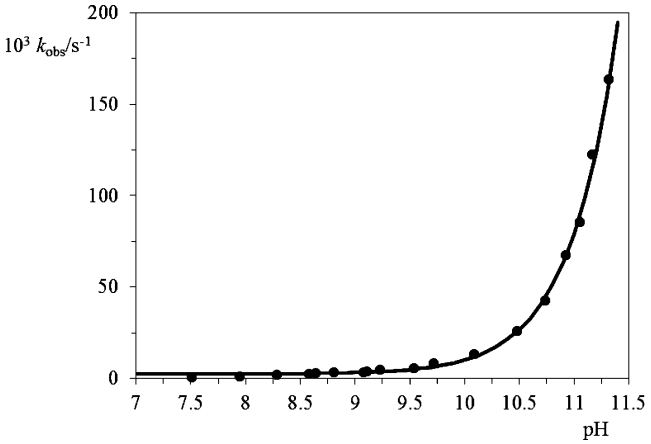

Figure 1. pH−rate profile in the BRB systems at 25 °C and I = 0.1 M.

From Figure 1, two distinct regions can be observed. The pH region 7.0−9.7 is characterized by the absence of any significant change in the k_{obs} values with the pH, which is consistent with the insignificant contribution of the parameter $k_{OH}[OH^-]$ from eq 4 to k_{obs}. Consequently, in this pH region OH^--independent β-elimination occurred. In contrast, in the pH region 10.7−11.3 a substantial increase in the k_{obs} values with increasing pH was observed, indicating an exclusive OH^--dependent β-elimination/hetero-Michael addition process. The evaluated kinetic parameters k_{Ac}, k_{HPO_4} and k_{OH} were 6.3×10^{-3}, 0.12, and 76.70 $M^{-1}\ s^{-1}$, respectively. Because the value of k_{OH} is expected to remain constant for different aqueous base systems at constant temperature and ionic strength, the value of 76.70 $M^{-1}\ s^{-1}$ was in excellent agreement with that obtained for the $OH^-/GLY^-/H_2O$ systems (85.0 $M^{-1}\ s^{-1}$). This result strongly supported the validity of the $(E1cb)_I$ mechanistic assignment of the rate-limiting β-elimination step in the overall rearrangement of **H-BEPA4** to **BEPyA4**.

Further evidence for the validity of the presented kinetic model was provided by computational analysis.

Computational Mechanistic Studies. The computational study was initiated by the analysis of the features of **H$_2$-BEPA4**$^+$. Its keto form is 8.9 kcal mol^{-1} more stable than the corresponding enol tautomer, suggesting that the ketone is the predominant form of **H$_2$-BEPA4**$^+$ in aqueous solution. The inspection of its acidity revealed that the solution-phase deprotonation free energy values, ΔG_{acid}, calculated for the reaction AH(sol) → A^-(sol) + H^+(sol) with the experimental value $\Delta G_{SOL}(H^+)$ = −265.9 kcal mol^{-1} [26] are 16.5, 27.0, and 33.8 kcal mol^{-1} for the deprotonation of the N−OH, α-CH_2, and β-CH_2 groups, respectively. This result indicated that the most acidic position in **H$_2$-BEPA4**$^+$ is the hydroxyl group of the oxime moiety. The calculated pK_{a1}(**H$_2$-BEPA4**$^+$)$_{oxime}$ value of 8.2 is in good agreement with the measured value of 8.51 ± 0.04 previously presented.[14] The first deprotonation of **H$_2$-BEPA4**$^+$ produces **H-BEPA4**, in which the keto form is even more favored over the enol by 9.7 kcal mol^{-1}. Considering the acidity of its two methylene groups, the calculated solution-phase ΔG_{acid} values for the α- and β-CH_2 sites are 31.0 and 52.5 kcal mol^{-1}, respectively. Interestingly, the value for the α-CH_2 group is only slightly different relative to **H$_2$-BEPA4**$^+$, whereas the β-CH_2 position becomes significantly less acidic. The second deprotonation produces **BEPA4**$^-$ and is associated with the calculated pK_{a2}(**H$_2$-BEPA4**$^+$)$_{\alpha\text{-}CH_2}$ value of 17.9. The latter value makes this position a few orders of magnitude more acidic than that in the simpler acetophenone (pK_a = 21.55)[27] and 2-propanone (pK_a = 19.3),[27] which is rationalized by the favorable inductive effect of the vicinal nitrogen within the piridinium moiety that facilitates deprotonation in **H-BEPA4**. During that process, the atomic charge on the mentioned nitrogen changes from −0.31 in **H$_2$-BEPA4**$^+$ to −0.36 in **BEPA4**$^-$.

In addition to the acid−base equilibria, the important prerequisite for the successful rearrangement of **H$_2$-BEPA4**$^+$ to **BEPyA4** in the proposed E1cb mechanism was the cleavage of the central C(β)−N$^+$(pyridinium) bond. We calculated the solution-phase free energies for the mentioned fragmentation through the homolytic and both of the heterolytic processes for **H$_2$-BEPA4**$^+$ (Scheme 3) and **H-BEPA4** and **BEPA4**$^-$ (Scheme 4). The three processes presented in Scheme 3 are associated with the reaction free energies that are excessively endergonic for an efficient reaction under normal conditions. The calculated

Scheme 3. Calculated Reaction Free Energy Values for the Cleavage of the Central C(β)−N$^+$(pyridinium) Bond in H$_2$-BEPA4$^+$

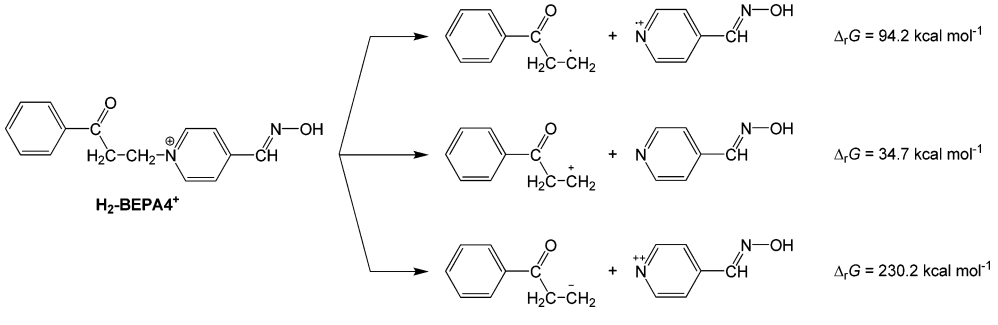

DOI: 10.1021/jo5026755
J. Org. Chem. 2015, 80, 2165−2173

Scheme 4. Calculated Reaction Free Energies for the Cleavage of the Central C(β)−N$^+$(pyridinium) Bond in BEPA4$^-$

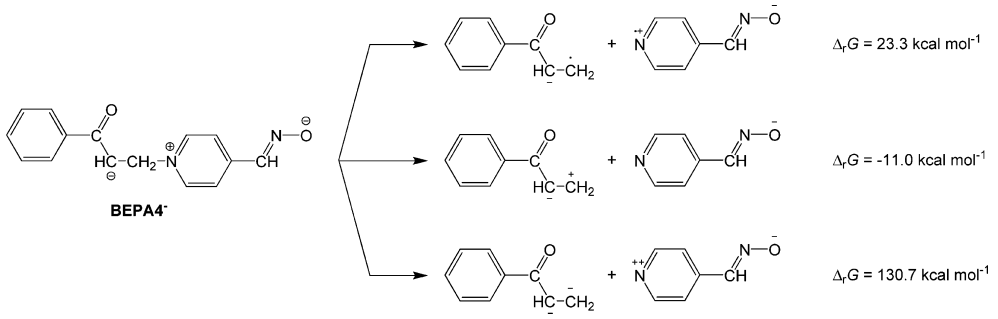

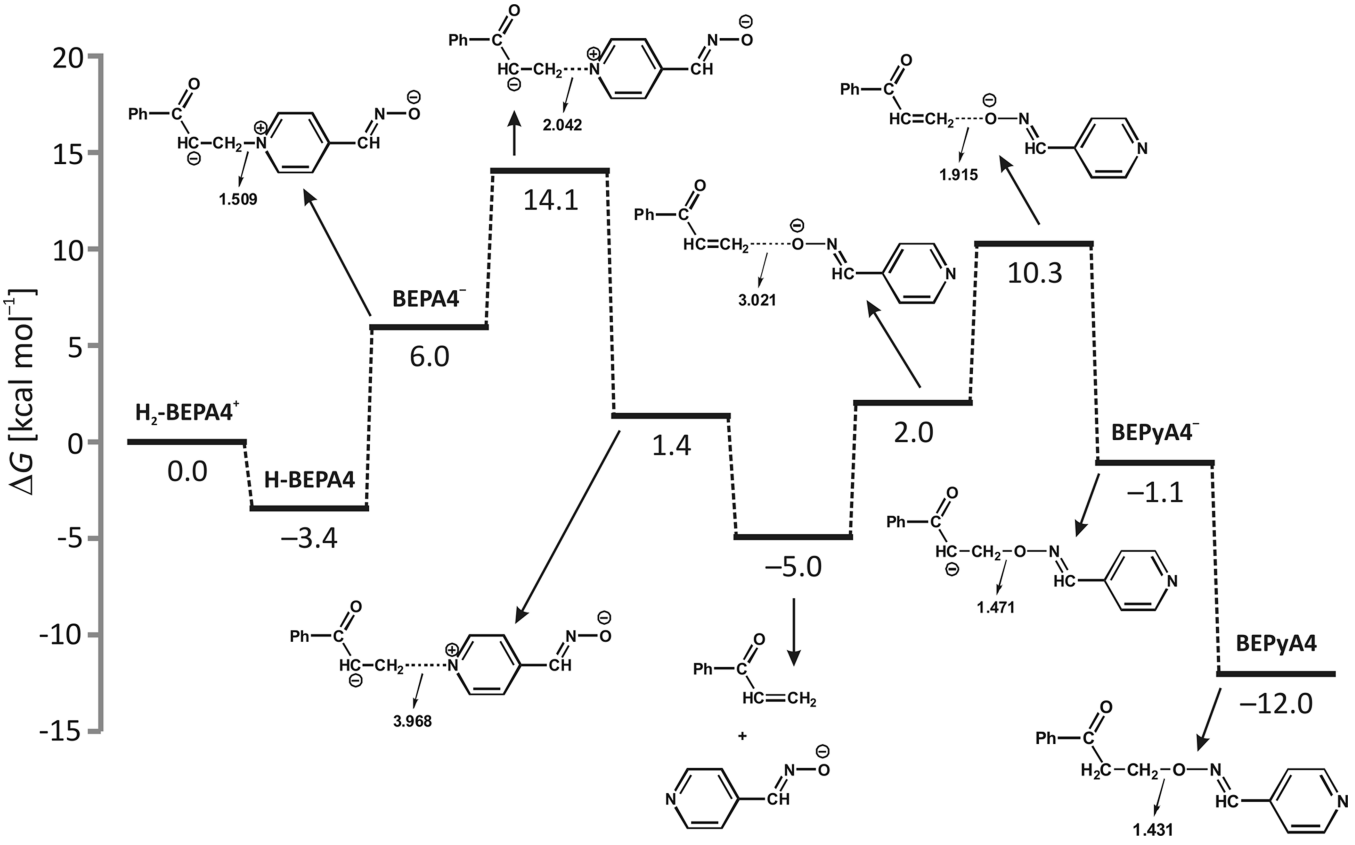

Figure 2. Free energy profile for the rearrangement of **H$_2$-BEPA4$^+$** to **BEPyA4** at a pH of 11, obtained by the (CPCM)/M06-2X/6-311++G(2df,2pd)//(CPCM)/ M06-2X/6-31+G(d,p) model. All of the relevant bond distances are given in Å.

$\Delta_r G$ values for the analogous bond cleavages in **H-BEPA4** were 41.1, 46.0, and 126.2 kcal mol^{-1}, respectively, and although two values are significantly reduced relative to those found in **H$_2$-BEPA4$^+$**, the calculated endergonicity for the most feasible process in **H-BEPA4** makes its decomposition even less likely to occur. Therefore, we considered the free energy requirements for the central C(β)−N$^+$(pyridinium) bond cleavage in **BEPA4$^-$** presented in Scheme 4.

Interestingly, the value for the heterolytic process resulting in **PVK** and **PyA4$^-$** is exergonic with a $\Delta_r G$ value of −11.0 kcal mol^{-1}, making this process thermodynamically spontaneous, being attributed to the resonance stabilization of the formed α-CH anionic center in **BEPA4$^-$**, which weakens the neighboring C(β)−N$^+$(pyridinium) bond. This stabilization is evident in the geometry changes as the C(α)−C(β) bond is shortened from 1.524 to 1.485 Å, whereas the C(β)−N$^+$(pyridinium) bond elongates from 1.472 to 1.509 Å upon deprotonation from **H-BEPA4** to **BEPA4$^-$**. We also noted that the corresponding C(α)−C(carbonyl) bond undergoes an even more significant change by shortening from 1.517 to 1.382 Å. Accordingly, this is well matched by the charge redistribution, as the atomic charges on the C(α), C(β), C(carbonyl), and O(carbonyl) atoms are −0.59, −0.27, 0.60, and −0.60 in **H-BEPA4**, while they are −0.54, −0.29, 0.39, and −0.86 in **BEPA4$^-$**, respectively.

The computational results presented suggest that the **H$_2$-BEPA4$^+$** and **H-BEPA4** forms are stable with respect to the cleavage of the central C(β)−N$^+$(pyridinium) bond. However, an increase in the pH of the solution enables the second deprotonation to **BEPA4$^-$**, which could undergo the mentioned fragmentation. Therefore, the investigation of the free energy profile for the complete rearrangement reaction starting from **H$_2$-BEPA4$^+$** and proceeding through **BEPA4$^-$** was required. The obtained results are presented in Figure 2 and are calculated for the aqueous solution at pH 11.0.

DOI: 10.1021/jo5026755
J. Org. Chem. 2015, 80, 2165−2173

The measured first and the calculated second pK_a values for **H_2-BEPA4$^+$** of pK_{a1} = 8.51 and pK_{a2} = 17.9 indicate that, at pH 11.0, the first deprotonation to **H-BEPA4** is spontaneous (ΔG = −3.4 kcal mol^{-1}), while the formation of a doubly deprotonated **BEPA4$^-$** occurs with the free energy cost of ΔG = 9.4 kcal mol^{-1} (Figure 2). From this point, 8.1 kcal mol^{-1} is required to arrive at the transition state for the cleavage of the C(β)−N$^+$(pyridinium) bond, characterized by one imaginary frequency of 235i cm^{-1}, thus leading to the total activation free energy of $\Delta G^{\ddagger}$ = 17.5 kcal mol^{-1}. During that process, the length of the mentioned bond increases from 1.509 to 2.042 Å and even further to 3.968 Å in the reaction intermediate, accompanied by a change in the atomic charges of C(β) and N$^+$(pyridinium) atoms from −0.29 and −0.36 to −0.35 and −0.54, respectively. Separation of the latter to the **PVK** and **PyA4$^-$** is thermodynamically favored, leading to a state that is more stable than the initial **H_2-BEPA4$^+$** ($\Delta_r G$ = −5.0 kcal mol^{-1}). The measured pK_a(**H-PyA4**) value of 9.99[17] implies that, at pH 11.0, the **PyA4$^-$** form predominates. This supports our mechanistic proposal, because our calculations suggest that **H-PyA4** is not sufficiently nucleophilic for the subsequent addition to **PVK**, since the resulting adduct decomposes into its components. This observation explains why the following Michael addition leading to **BEPyA4** occurs only in more alkaline media (pH >10.0). However, the formation of the reactive complex for the nucleophilic addition of **PyA4$^-$** to **PVK** requires 7.0 kcal mol^{-1} and an additional 8.3 kcal mol^{-1} to arrive at the transition state for the C(β)−O$^-$(oximate) bond formation, characterized by an imaginary frequency of 305i cm^{-1}. The activation free energy for the second step is therefore $\Delta G^{\ddagger}$ = 15.3 kcal mol^{-1}, and the reaction results in the formation of **BEPyA4$^-$**. At pH 11.0, **BEPyA4$^-$** reprotonates (with a calculated pK_a(**BEPyA4**)$_{\alpha\text{-}CH_2}$ value of 19.0), with a gain in energy of ΔG = −10.9 kcal mol^{-1}, to give **BEPyA4** as the final product, being more stable by 12.0 kcal mol^{-1} than the initial **H_2-BEPA4$^+$**. The latter value and the complete free energy profile (Figure 2) suggest that the tandem β-elimination/hetero-Michael addition rearrangement is thermodynamically favorable and is a feasible process. Furthermore, it appears that the first step, the β-elimination involving **H_2-BEPA4$^+$** to **BEPA4$^-$** deprotonation and C(β)−N$^+$(pyridinium) bond cleavage, represents the rate-limiting step of the overall rearrangement with a $\Delta G^{\ddagger}$ value of 17.5 kcal mol^{-1}, which is in excellent agreement with the reported experimental value of 18.8 kcal mol^{-1} (Table 1). Additionally, the computational data for $\Delta G^{\ddagger}$ at the pH values of 10.0, 10.5, and 11.5 were 18.8, 18.2, and 16.8 kcal mol^{-1}, respectively, which agree with the experimental values of 20.9, 19.6, and 18.2 kcal mol^{-1} (Table 1), respectively. These results provide strong support for the proposed reaction mechanism of the tandem β-elimination/hetero-Michael addition rearrangement. In concluding this section, we mention that we also studied two alternative mechanisms for the investigated rearrangement: namely, (a) nucleophilic addition of the −CH═NOH group to the β-CH$_2$ moiety between two **H_2-BEPA4$^+$** ions and (b) the same reaction involving the −CH═NO$^-$ group between two **H-BEPA4** systems. The first reaction did not produce the stable reactive complex between the two molecules, whereas the second process is feasible, but the calculated $\Delta G^{\ddagger}$ value is significantly higher than that in the proposed reaction mechanism.

CONCLUSIONS

We introduced a new reaction pathway, an intramolecular tandem β-elimination/hetero-Michael addition reaction sequence, for the synthesis of O-alkylated pyridine oxime ether by the rearrangement of the corresponding N-alkylated pyridinium oxime in an alkaline aqueous solution. This rearrangement process was pH-dependent i.e., controlled by the concentration of *N*-benzoylethylpyridinium-4-oximate which is the ionic form susceptible to β-elimination, and pyridine-4-oximate which is a strong oxygen nucleophile and therefore an excellent Michael donor. The combined experimental and computational mechanistic studies revealed the general-base-catalyzed reaction mechanism with β-elimination as the rate-limiting reaction step. Detail mechanistic inspection of the β-elimination provided evidence that supports an $(E1cb)_I$ mechanism that includes the following two elementary reactions: rate-limiting, base-induced formation of carbanion and its rapid decomposition.

To the best of our knowledge, the mentioned rearrangement represents the first example of a tandem reaction in which the leaving group produced by the β-elimination becomes a reactive Michael donor group. Additionally, these results provide useful guidelines for further synthetic studies to establish a new and operationally simple, metal-free, one-stage experimental protocol for the synthesis of O-alkylated pyridine oxime ethers in aqueous media.

EXPERIMENTAL SECTION

General Procedures. The elemental analysis was performed with an analyzer, using the Active Standard Test Method D 5291. The melting point was determined on a calorimeter with a temperature accuracy of ±0.2 °C. The FT-IR spectra were recorded over the range 4000−400 cm^{-1} using KBr pellets. The single mass analysis was obtained with a mass spectrometer using electrospray ionization. The kinetic measurements were performed on a spectrophotometer with a thermostated cell holder and 1 cm silica glass cells. The ^{1}H MAS and ^{13}C CP-MAS NMR spectra were recorded on a 600 MHz NMR spectrometer equipped with a 3.2 mm NB Double-Resonance HX MAS Solids Probe and were externally referenced using adamantane and hexamethylbenzene, respectively. The Larmor frequencies of the protons and the carbon nuclei were 599.77 and 150.83 MHz, respectively. The ^{1}H, ^{13}C, gCOSY, ^{1}H−^{13}C gHSQC, ^{1}H−^{13}C gHMBC, and ^{1}H−^{15}N gHMBC NMR spectra were recorded with a spectrometer operating at 600.133 MHz for hydrogen and 150.917 MHz for the carbon nuclei. The solvent signals were used as the internal standards, which were related to TMS (δ 0 ppm) with δ 2.49 ppm (^{1}H, [D$_6$]DMSO) and δ 39.5 ppm (^{13}C, [D$_6$]DMSO). The abbreviations used were as follows: s, singlet; d, doublet; dd, doublet of doublets; t, triplet; m, multiplet.

Deionized water was used throughout all of the experiments and measurements. The Britton−Robinson buffer systems were prepared by combining a mixture of 0.04 M solutions of phosphoric, boric, and acetic acid (20 mL) with different volumes of 0.20 M sodium hydroxide solution. All of the other reagents employed were commercially available high-purity materials, which were used as supplied without further purification.

(*E*)-*N*-Benzoylethylpyridinium-4-oxime Chloride (H_2-BEPA4$^+$Cl$^-$**).** The preparation procedure, spectroscopic characterization (FT-IR, FT-Raman, FT-MS, ^{1}H and ^{13}C NMR), and crystal structure parameters have been provided in a previous study.[14] Because of their relevance, the ^{1}H and ^{13}C NMR chemical shifts, readjusted to the numeration presented in Scheme 1, are cited in this study.[16] ^{1}H−^{15}N gHMBC NMR (600 MHz, [D$_6$]DMSO, 25 °C, TMS): δ 405.10 (CH═N), 210.03 (PyN$^+$) ppm. Anal. Calcd for $C_{15}H_{15}N_2O_2Cl$: C, 61.97; H, 5.20; N, 9.64. Found: C, 61.95; H, 5.23; N, 9.73.

(*E*)-*O*-Benzoylethylpyridine-4-oxime (BEPyA4). (*E*)-*O*-Benzoylethylpyridine-4-oxime was precipitated by the addition of a sodium hydroxide solution (15.0 mL, 0.2 M) to an aqueous solution (30 mL) of (*E*)-*N*-benzoylethylpyridinium-4-oxime chloride (1.018 g, 3.5 mmol). (*E*)-*O*-Benzoylethylpyridine-4-oxime was obtained as a white powder by

DOI: 10.1021/jo5026755
J. Org. Chem. 2015, 80, 2165−2173

Table 3. Characteristic Electronic Absorption Bands of the Predominant Forms of BEPyA4 in Aqueous Solutions and the Ionization Constant at 25 °C and I = 0.1 M

λ_{max}/nm	band assignt[a]	ε(**H-BEPyA4**$^+$) (dm^3 mol^{-1} cm^{-1})	ε(**BEPyA4**) (dm^3 mol^{-1} cm^{-1})	pK_a(**H-BEPyA4**$^+$)
252	K(acetophenone)	18860		4.65 ± 0.14
251	K(acetophenone), ^1L_b(py−CH═NOR)		26190	
284	^1L_b (acetophenone), ^1L_b(py$^+$−CH═NOR)	19570		

[a]The band assignation was made according to the Klevens−Platt nomenclature.

recrystallization from a water−ethanol mixture (0.356 g, 40.0%). Mp: 87.8 °C. ^{1}H NMR (600.133 MHz, [D$_6$]DMSO, 25 °C, TMS): δ 8.60 (d, J = 5.94 Hz, 2H, H2, H6; PyH), 8.22 (s,1H, CH═N), 7.99 (d, J = 7.20 Hz, 2H, H11, H15; ArH), 7.58 (t, J = 7,38 Hz, 1H, H13; ArH), 7.47 (t, J = 7.71 Hz, 2H, H12, H14; ArH), 7.40 (d, J = 5.88 Hz, 2H, H3, H5; PyH), 4.56 (t, J = 6.33 Hz, 2H, H7; CH$_2$), 3.47 (t, J = 6.30 Hz, 2H, H8; CH$_2$). ^{13}C NMR (150.197 MHz, [D$_6$]DMSO, 25 °C, TMS): δ 197.8 (C9; C═O), 150.2 (C2, C6; PyC), 147.3 (CH═N), 139.0 (C4; PyC), 136.5 (C10; ArC), 133.3 ppm (C13; ArC), 128.7 (C12, C14; ArC), 128.0 (C11, C15; ArC), 120.8 (C3, C5; PyC), 69.8 (C7; CH$_2$), 37.5 (C8; CH$_2$). ^{13}C CP-MAS NMR: δ 151.0 (C2, C6; PyC), 116.1 (C3, C5; PyC), 144.4 (C4; PyC), 164.2 (CH═N), 71.0 (C7; CH$_2$), 36.4 (C8; CH$_2$), 197.0 (C9; C═O), 136.6 (C10; ArC), 123.5 (C11, C15; ArC), 130.8 (C12, C14; ArC), 133.4 (C13; ArC) ppm. ^{1}H−^{15}N gHMBC NMR (600 MHz, [D$_6$]DMSO, 25 °C, TMS): δ 392.2 (CH═N), 320.1 (PyN) ppm. FT-IR (KBr): $\tilde{\nu}$ 3052, 2967, 2904, 1674, 1598, 1581, 1552, 1456, 1218, 1046, 954, 532 cm^{-1}. MS (ESI-Q-Tof): m/z [M + H]$^+$ calcd for $C_{15}H_{14}N_2O_2$, 255.1128; found, 255.1135; Anal. Calcd for $C_{15}H_{14}N_2O_2$: C, 70.85; H, 5.55; N, 11.02. Found: C, 70.75; H, 5.70; N, 10.91.

UV/vis Characterization of BEPyA4 in BRB Aqueous Solutions. The electron absorption spectra were composed of pH-dependent electronic absorption bands that clearly defined the equilibrium between **H-BEPyA4**$^+$ and **BEPyA4** (Table 3). The pK_a(**H-BEPyA4**$^+$) values were evaluated spectrophotometrically at 25 °C and I = 0.1 M from the absorbance vs pH data by the general method given by Albert and Serjeant.[28] The K_a, A(**H-BEPyA4**$^+$), and A(**BEPyA4**) values were computed by fitting the measured absorbances (A) at 251 and 284 nm, respectively, as a function of pH (Figure S5 (Supporting Information)) according to eq 5.

$$A = \frac{[A(\mathrm{HL})]10^{-\mathrm{pH}} + [A(\mathrm{L})]K_a}{10^{-\mathrm{pH}}K_a} \quad (5)$$

Identification of the Reactive Intermediates. (*E*)-*N*-Benzoylethylpyridinium-4-oxime chloride (**H$_2$-BEPA4$^+$Cl$^-$**; 100 mg, 0.34 mmol) was dissolved in BRB solutions at pHs of 10.1, 10.5, and 11.1 (6.0 mL). The reaction mixtures were allowed to equilibrate at ambient temperature for 2 h. After removal of the water by lyophilization, the residual mixtures were dissolved in [D$_6$]DMSO and the ^{1}H and ^{13}C NMR spectra were recorded. The obtained chemical shifts are identified and presented in Table S1 (Supporting Information).

Kinetic Studies. The rearrangement of **H-BEPA4** to **BEPyA4** was followed by spectrophotometric monitoring of the absorbance decrease of the **H-BEPA4** charge-transfer band at 340 nm. The reactions followed first-order kinetics for at least 2 half-lives, and the observed pseudo-first-order rate constants, k_{obs}, were determined. A standard kinetic experiment was performed by injecting a freshly prepared stock solution of **H$_2$-BEPA4$^+$Cl$^-$** into a thermally equilibrated reaction solution contained in a cuvette, yielding a final **H$_2$-BEPA4$^+$** concentration of 1.0 × 10^{-5} M. The kinetic runs were started immediately after the stock solutions were added. In all of the kinetic solutions, the ionic strength was maintained at 0.1 M by the addition of a NaCl solution. All of the measurements were performed at least in triplicate. The thermal activation parameters were determined from the Eyring linear plots of ln(k_{obs}/T) vs 1/T over the temperature range of 10−25 °C (Table S2 and Figures S6 and S7 (Supporting Information)). The effect of the buffer concentration on the reaction rate was established by varying the buffer base concentration from 6.22 ×10^{-3} to 1.24 × 10^{-1} M with a constant [GLY$^-$]/[GLYH] ratio at 25 °C and I = 0.1 M. Two sets of glycine buffer systems of pH 9.80 and 10.30 were prepared by dissolving glycine (0.050, 0.075, 0.250, 0.500, and 1.000 g for pH 9.80 and 0.031, 0.047, 0.157, 0.312, and 0.624 g for pH 10.30) in water and by adding a 0.2 M solution of NaOH (1.67, 2.50, 8.33, 16.65, and 33.25 mL). For the diluted buffer solutions, the pH values were adjusted to the pH value measured for the highest buffer concentration by the addition of negligible volumes of a 0.1 M HCl or 0.2 M NaOH solution. The pHs of the reaction mixtures were measured after completion of the kinetic runs. The kinetic runs exhibited a maximal pH drift of ±0.04.

Computational Details. As a good compromise between accuracy and computational feasibility, all of the molecular geometries were optimized by the efficient M06-2X/6-31+G(d,p) model. The thermal Gibbs free energy corrections were extracted from the corresponding frequency calculations without the application of scaling factors. The final single-point energies were attained with a highly flexible 6-311++G(2df,2pd) basis set using the M06-2X functional, which was designed by Truhlar's group to provide highly accurate thermodynamic and kinetic parameters for organic systems, being particularly successful in treating nonbonding interactions[29] without underestimating the reaction barrier, which occurs in many other DFT approaches. Several recent review articles have emphasized this method's excellent accuracy in this respect.[30] To account for the effects of the aqueous solution we included, during the geometry optimization and the single-point energy evaluation, a conductor-like polarizable continuum model (CPCM)[31] with all of the parameters for pure water, giving rise to the (CPCM)/M06-2X/6-311++G(2df,2pd)//(CPCM)/M06-2X/6-31+G(d,p) model employed in this study. All of the transition state structures were verified to have the appropriate imaginary frequencies, from which the corresponding reactants and products were determined using the intrinsic reaction coordinate (IRC) procedure.[32] Atomic charges were obtained through the natural bond orbital (NBO) analysis at the (CPCM)/M06-2X/6-31+G(d,p) level. All of the reported relative pK_a values were calculated using the (SMD)/M06-2X/6-311++G-(2df,2pd)//(SMD)/M06-2X/6-31+G(d,p) model employing pyridinium-4-oxime (pK_a = 8.51)[27] and acetophenone (pK_a = 21.55)[27] as the reference acids for the investigated deprotonations of the oxime and α-methylene groups, respectively. All of the calculations were performed using the Gaussian 09 software.[33]

■ ASSOCIATED CONTENT

Supporting Information

Tables and figures giving FT-IR and ^{1}H and ^{13}C NMR spectra for **BEPyA4**, ^{1}H and ^{13}C NMR chemical shifts of the reaction participants obtained at different pHs, values of the observed pseudo-first-order rate constants, linear plots of k_{obs} (s^{-1}) vs OH$^-$ and GLY$^-$concentrations, Eyring plots, pH dependence of the absorbance of **BEPyA4** on pH, Cartesian coordinates and total molecular energies of all computationally investigated systems, and selected geometric parameters and NBO atomic charges of all compounds along the reaction pathway. This material is available free of charge via the Internet at http://pubs.acs.org.

■ AUTHOR INFORMATION

Corresponding Authors

*E-mail for I.P.: ipicek@mef.hr.

*E-mail for R.V.: Robert.Vianello@irb.hr.

DOI: 10.1021/jo5026755
J. Org. Chem. 2015, 80, 2165−2173

*E-mail for B.F.: bforetic@mef.hr.

Notes

The authors declare no competing financial interest.

■ ACKNOWLEDGMENTS

Financial support for this research was provided by the Ministry of Science, Education and Sports of the Republic of Croatia (Grant Nos. 108-1193079-3070 and 098-0982933-2932) and by the Slovenian Research Agency (ARRS, grants P1-0242 and J1-6733). R.V. gratefully acknowledges the European Commission for an individual FP7 Marie Curie Career Integration Grant (Contract No. PCIG12-GA-2012-334493). We are very grateful to Dr. Bogdan Kralj for mass spectrometry measurements. I.P. wishes to thank Prof. Nicoletta Burger for her support and helpful discussions.

■ REFERENCES

(1) Mancin, F.; Tecilla, P.; Tonellato, U. *Langmuir* **2000**, *16*, 227−233.
(2) Jokanović, M. *Curr. Top. Med. Chem.* **2012**, *16*, 1775−1789 and references cited therein.
(3) Acharya, J.; Gupta, A. K.; Dubey, D. K.; Raza, S. K. *Eur. J. Med. Chem.* **2009**, *44*, 1335−1340 and references cited therein.
(4) Bhandari, K.; Srinivas, N.; Keshava, G. B. S.; Shukla, P. K. *Eur. J. Med. Chem.* **2009**, *44*, 437−447.
(5) Johnson, S. M.; Petrassi, H. M.; Palaninathan, S. K.; Mohamedmohaideen, N. N.; Purkey, H. E.; Nichols, C.; Chiang, K. P.; Walkup, T.; Sacchettini, J. C.; Sharpless, K. B.; Kelly, J. W. *J. Med. Chem.* **2005**, *48*, 1576−1587.
(6) Abele, E.; Abele, R.; Arsenyan, P.; Shestakova, I.; Kanepe, I.; Antonenko, I.; Popelis, J.; Lukevics, E. *Bioinorg. Chem. Appl.* **2003**, *1*, 299−308.
(7) Abele, E.; Abele, R.; Lukevics, E. *Chem. Heterocycl. Compd.* **2003**, *39*, 825−865 and references cited therein.
(8) Cao, Z.; Liu, Z.; Liu, Y.; Du, H. *J. Org. Chem.* **2011**, *76*, 6401−6406 and references cited therein.
(9) Pohjakallio, A.; Pihko, P. M.; Laitinen, U. M. *Chem. Eur. J.* **2010**, *16*, 11325−11339.
(10) Miyabe, H.; Matsumura, A.; Yoshida, K.; Takemoto, Y. *Tetrahedron* **2009**, *65*, 4464−4470 and references cited therein.
(11) Jin, J.; Li, Y.; Wang, Z.; Qian, W.; Bao, W. *Eur. J. Org. Chem.* **2010**, 1235−1238.
(12) Gaspar, B.; Carreira, E. M. *J. Am. Chem. Soc.* **2009**, *131*, 13214−13215.
(13) Foretić, B.; Picek, I.; Damjanović, V.; Cvijanović, D.; Pulić, I.; Kukovec, B. M.; Matković-Čalogović, D. *Polyhedron* **2013**, *52*, 733−742.
(14) Foretić, B.; Picek, I.; Damjanović, V.; Cvijanović, D.; Milić, D. *J. Mol. Struct.* **2012**, *1019*, 196−205.
(15) Visser, R.; Dahmen, E. A. M.F. *Anal. Chim. Acta* **1978**, *100*, 271−277.
(16) Cited from ref 14. ^{1}H NMR (600 MHz, [D_6]DMSO, 25 °C, TMS): δ 9.15 (d, J = 6.78 Hz, 2H, H2, H6; PyH), 8.24 (d, J = 6.78 Hz, 2H, H3, H5; PyH), 4.95 (t, J = 6.54 Hz, 2H, H7; CH_2), 3.96 (t, J = 6.54 Hz, 2H, H8; CH_2), 7.97 (d, J = 7.20 Hz, 2H, H11, H15; ArC), 7.56 (t, J = 7.77 Hz, 2H, H12, H14; ArC), 7.68 (t, J = 7.38 Hz, 1H, H13; ArC), 8.43 (s, 1H, CH═N), 12.93 (s, 1H, OH) ppm. ^{13}C NMR (150 MHz, [D_6] DMSO, 25 °C, TMS): δ 145.8 (C2, C6; PyC), 123.8 (C3, C5; PyC), 148.6 (C4; PyC), 55.8 (C7; CH_2), 38.9 (C8; CH_2), 197.0 (C9; C═O), 135.9 (C10; ArH), 128.1 (C11, C15; ArH), 128.9 (C12, C14; ArH), 133.9 (C13; ArH), 145.1 (CH═N) ppm.
(17) Mason, S. F. *J. Chem. Soc.* **1960**, 22−26.
(18) Alunni, S.; Laureti, V.; Ottavi, L.; Ruzziconi, R. *J. Org. Chem.* **2003**, *68*, 718−725.
(19) Alunni, S.; Ottavi, L. *J. Org. Chem.* **2004**, *69*, 2272−2283.
(20) Keeffe, J. R.; Jencks, W. P. *J. Am. Chem. Soc.* **1983**, *105*, 265−279.
(21) Bunting, J. W.; Toth, A.; Kanter, J. P. *Can. J. Chem.* **1992**, *70*, 1195−1203.
(22) Cox, B. G.; De Maria, P.; Fini, A.; Hassan, A. F. *J. Chem. Soc., Perkin Trans. 2* **1981**, 1351−1357.
(23) Because the value of the second **H_2-BEPA4$^+$** ionization constant was estimated as $K_{a2}(\mathbf{H_2\text{-}BEPA4^+})_{\alpha\text{-}CH_2} < 10^{-12}$,[14] the value of 6.3 × 10^{-19} M was calculated from the following expression: $pK_{a2}(H_2\text{-}BEPA4^+)_{\alpha\text{-}CH_2} = pK_{a1}(\mathbf{H_2\text{-}BEPA4^+})_{oxime}]_{exp} + [pK_{a2}(\mathbf{H_2\text{-}BEPA4^+})_{\alpha\text{-}CH_2} - pK_{a1}(\mathbf{H_2\text{-}BEPA4^+})_{oxime}]_{theor.calcd}$, where $pK_{a1}(\mathbf{H_2\text{-}BEPA4^+})_{oxime}$ is 8.51[8] and $[pK_{a2}(\mathbf{H_2\text{-}BEPA4^+})_{\alpha\text{-}CH_2} - pK_{a1}(\mathbf{H_2\text{-}BEPA4^+})_{oxime}]_{theor.calcd}$ is 9.7 (see Computational Mechanistic Studies).
(24) Alunni, S.; De Angelis, F.; Ottavi, L.; Papavasileiou, M.; Tarantelli, F. *J. Am. Chem. Soc.* **2005**, *127*, 15151−15160.
(25) Richard, P.; Williams, G.; Gao, J. *J. Am. Chem. Soc.* **1999**, *117*, 715−726.
(26) Tissandier, M. D.; Cowen, K. A.; Feng, W. Y.; Gundlach, E.; Cohen, M. H.; Earhart, A. D.; Coe, J. V.; Tuttle, T. R., Jr. *J. Phys. Chem. A* **1998**, *102*, 7787−7794.
(27) Jencks, W. P.; Regenstein, J. Ionization constants of acids and bases. In *Handbook of Biochemistry and Molecular Biology*; Fasman, G. D., Ed.; CRC Press: Cleveland, OH, 1976; pp 305−351.
(28) Albert, A.; Serjeant, E. P. *The Determination of Ionization Constants*; Chapman and Hall: London, 1971; pp 44−64.
(29) (a) Zhao, Y.; Truhlar, D. G. *Theor. Chem. Acc.* **2008**, *120*, 215−241. (b) Zhao, Y.; Truhlar, D. G. *J. Chem. Theory Comput.* **2011**, *7*, 669−676. (c) Zhao, Y.; Truhlar, D. G. *Acc. Chem. Res.* **2008**, *41*, 157−167.
(30) (a) Cohen, A. J.; Mori-Sánchez, P.; Yang, W. *Chem. Rev.* **2012**, *112*, 289−320. (b) Cheong, P. H.-Y.; Legault, C. Y.; Um, J. M.; Çelebi-Ölçüm, N.; Houk, K. N. *Chem. Rev.* **2011**, *111*, 5042−5137. (c) Bell, A. T.; Head-Gordon, M. *Annu. Rev. Chem. Biomol. Eng.* **2011**, *2*, 453−477.
(31) Cossi, M.; Rega, N.; Scalmani, G.; Barone, V. *J. Comput. Chem.* **2003**, *24*, 669−681.
(32) Fukui, K. *Acc. Chem. Res.* **1981**, *14*, 363−368.
(33) Frisch, M. J.; Trucks, G. W.; Schlegel, H. B.; Scuseria, G. E.; Robb, M. A.; Cheeseman, J. R.; Scalmani, G.; Barone, V.; Mennucci, B.; Petersson, G. A.; Nakatsuji, H.; Caricato, M.; Li, X.; Hratchian, H. P.; Izmaylov, A. F.; Bloino, J.; Zheng, G.; Sonnenberg, J. L.; Hada, M.; Ehara, M.; Toyota, K.; Fukuda, R.; Hasegawa, J.; Ishida, M.; Nakajima, T.; Honda, Y.; Kitao, O.; Nakai, H.; Vreven, T.; Montgomery, J. A., Jr.; Peralta, J. E.; Ogliaro, F.; Bearpark, M.; Heyd, J. J.; Brothers, E.; Kudin, K. N.; Staroverov, V. N.; Kobayashi, R.; Normand, J.; Raghavachari, K.; Rendell, A.; Burant, J. C.; Iyengar, S. S.; Tomasi, J.; Cossi, M.; Rega, N.; Millam, J. M.; Klene, M.; Knox, J. E.; Cross, J. B.; Bakken, V.; Adamo, C.; Jaramillo, J.; Gomperts, R.; Stratmann, R. E.; Yazyev, O.; Austin, A. J.; Cammi, R.; Pomelli, C.; Ochterski, J. W.; Martin, R. L.; Morokuma, K.; Zakrzewski, V. G.; Voth, G. A.; Salvador, P.; Dannenberg, J. J.; Dapprich, S.; Daniels, A. D.; Farkas, Ö.; Foresman, J. B.; Ortiz, J. V.; Cioslowski, J.; Fox, D. J. *Gaussian 09, Revision A.02*; Gaussian, Inc., Wallingford, CT, 2009.

■ NOTE ADDED AFTER ASAP PUBLICATION

After this paper was published ASAP January 23, 2015, the value for $\Delta_r G$ for **H2-BEPA4$^+$** in the Computational Mechanistic Studies section was corrected. The corrected version was reposted January 30, 2015.

DOI: 10.1021/jo5026755
J. Org. Chem. 2015, 80, 2165−2173